Proceedings of CONF-MCEE 2026 Symposium: Geomaterials and Environmental Engineering
DOI: 10.54254/2755-2721/2026.MH30175

Ion Migration Mechanism and Regulation Technology of Perovskite Photovoltaic Devices

Tianyou Huang[1*†], Jiuxuan Xu[1†]

[1]*Beijing National Day School, Beijing, China*
**Corresponding Author. Email: tianyou.huang@hotmail.com*
[†]*These authors contributed equally to this work and should be considered as co-first author.*

Abstract. Current global energy problems call for the development of efficient, environmentally friendly and sustainable energy sources. Among them, solar power, harvested by emerging organic-inorganic hybrid perovskite (PVK) materials is among the most promising research aim. The precise evaluation of power conversion efficiency (PCE), a crucial part in understanding the performance of photovoltaic cells, is significantly hindered by ion migration in PVK. In this study, we explored the impact of partial substitution of methylammonium (MA+) with formamidinium (FA+) on perovskite films. We discovered that the incorporation of large size cations in PVK inhibits ion migration in those devices, due to steric hindrance. This modification led to enhanced performance, with modified cells showing increased light absorption efficiency exceeding 800 nm and a higher mean and median power conversion efficiency. Such discovery lies the foundation of a reliable method to have a comprehensive understanding of the essence of ion migration and a method on how to regulate them.

Keywords: Organic-inorganic Perovskite, Photovoltaic Device, Ion Migration, Steric Effect, Open Circuit Voltage Decay

1. Introduction

1.1. Development and application background of PVK technology

The current energy crisis, as well as the global warming problem, calls for the development of sustainable and carbon-free energy sources. Perovskite materials (chemical formula ABX3, as shown in Figure 1), first applied to solar cells in 2009, are among the advanced solutions. Their efficiency in converting solar power to electricity has increased from 3.8% [1] to 26.9% in 2025 [2]. This value matches monocrystalline silicon batteries (about 27.8%) and surpasses traditional thin film batteries (about 23.6%) [3]. Its advantages lie in 1) low-cost processing techniques at low temperatures (<150 ℃), and 2) tunability of its light absorption spectrum by adjusting ions at positions A, B and X [4, 5]. For example, the initial wavelength of maximum light absorption of CH3NH3PbI3 is 825 nm (A=CH3NH3+, b=Pb2+, X=I−), and replacing CH3NH3+, Pb2+, and I− with FA+ and Br− forms FAPbIγBr3−γ and changes this wavelength between 556 nm and 838 nm. These characteristics make it a core material for energy conversion.

© 2026 The Authors. This is an open access article distributed under the terms of the Creative Commons Attribution License 4.0 (https://creativecommons.org/licenses/by/4.0/).

DOI: 10.54254/2755-2721/2026.MH30175

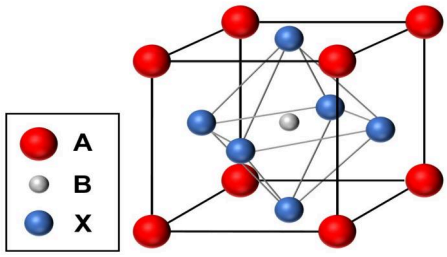


Figure 1. The ABX3 perovskite crystal structure

1.2. The influence of ion migration on perovskite cells

The commercialization of perovskite cells is hampered by their limited stability, in which ion migration is the main cause. The process of ion migration is illustrated in Figure 2. The results of ion migration in perovskite materials include lattice distortion [6], phase separation [7], and unwanted chemical reactions with other interfacial materials [8]. These behaviors lead to photocurrent hysteresis and efficiency attenuation. The efficiency of unencapsulated batteries was reported to drop significantly in hundreds of hours in the atmosphere [9].

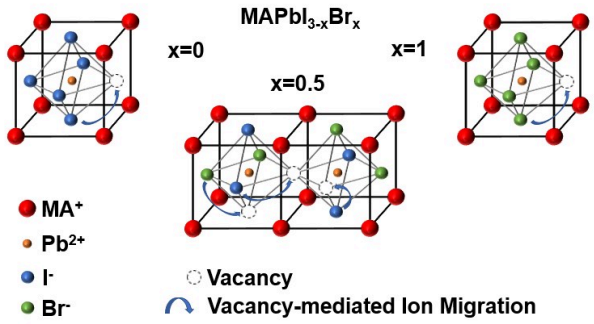


Figure 2. Schematic diagram of the ion migration process

The influence on the performance of perovskite photovoltaic devices includes two phenomena. In the unoptimized material, the migration rate resulted in a T80 lifetime of only 700 hours for the device [10]. Furthermore, ion migration promotes exciton decomposition under a local electric field and decreases the efficiency of the material. For example, regulation of the double interface dipole layer increases the efficiency to 26.1% [11]. Figure 3 summarizes several aspects of potential effects.

DOI: 10.54254/2755-2721/2026.MH30175

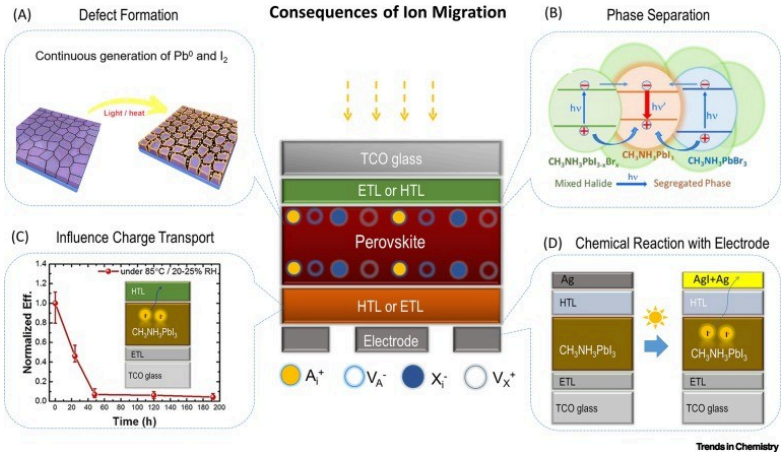


Figure 3. Consequences of ion migration [12]

1.3. Regulatory strategies and scientific significance of ion migration

The detection of ion migration in perovskite materials has long been the focus of several researchers [13-16]. Controlling and regulating ion migration in perovskite materials is of equal importance, as it relates not only to the improvement of device stability but also to performance optimization. Ion migration is a key factor in device degradation; by employing strategies such as interstitial doping, introducing buffer layers, or utilizing 2D layered structures to suppress ion migration, the device lifespan can be significantly extended. For example, the multi-iodide supramolecular buffer layer [17] and trace neodymium ion doping allowed the device to maintain high efficiency even after long-term operation. From a scientific perspective, 2D layered perovskites form a 'migration barrier', reducing the ion migration rate, and allowing the device to retain over 60% of its performance after 2250 hours of illumination [18].

Furthermore, controlling ion migration also improves device performance. Prof. Chang and coworkers introduced fluoride ions into perovskite materials to increase the rigidity of the lattice and unlock the application of such devices under extreme conditions [19]. Prof. He and coworkers utilized the host-guest interaction of calixarene supramolecules [20] to achieve similar effects. Advanced techniques such as in situ nano-infrared imaging (with a spatial resolution of 10 nm) and time-of-flight secondary ion mass spectrometry technology [8] provide powerful tools to track ion migration paths and volume phase distributions, facilitating in-depth research. In general, regulation of ion migration is a key factor in advancing perovskite materials from the laboratory to industrialization [21].

In the application, we incorporated large sized FA+ ion into PVK cells, using a high steric hindrance to obstruct the rate of ion migration. Using our results, one can understand the core factors affecting ion migration.

2. Material and experiments

2.1. Substrate cleaning

1.The fluoride tin oxide (FTO) substrate was cleaned sequentially with detergent, deionized water, acetone and alcohol in ultrasonic cleaner for 15 minutes twice.

2.The substrate was then let dried via nitrogen blow.

3.Plasma cleaning was performed for increased substrate surface wettability.

DOI: 10.54254/2755-2721/2026.MH30175

2.2. Electron transport layer coating

1.SnO2 was diluted with deionized water to make a 10% concentration solution.
2.The SnO2 solution was filtrated with a 0.22 μm membrane filter to remove insoluble particles.
3.90 μL SnO2 solution was dropped on the substrate for further spin coating at 200 rpm for 30 sec.
4.The substrate was annealed on a 150 ℃ heater for 30 minutes.

2.3. PVK active layer coating

2.3.1. Normal PVK active layer coating

1.PbI2 and MAI were measured with a molar ratio of 1:1.
2.DMF and DMSO were measured with a volume ratio of 7:3.
3.All measured reagents were dissolved in 1 mL solute and stirred overnight under 100 ℃.
4.All solutions were filtrated using 0.22 μm membrane filter.
5.60 μL of the precursor solution was dropped on the prepared substrate.
6.The substrate was then spun with 1000 rpm for 2 sec, then accelerated to 5000 rpm in 4 sec, the substrate was then spun with 5000 rpm for 34 sec.
7.The prepared PVK film was then heated at 100 ℃ for 10 minutes.

2.3.2. Modified PVK active layer coating

1.PbI2, MAI and FAI were measured with a molar ratio of 1:0.15:0.85.
2.Steps were repeated from 2.3.1 from step 2.

2.4. Hole Transport Layer (HTL) coating

1.A 73.2 μg/mL Spiro-OMeTAD chlorobenzene solution was made.
2.8.8 μL lithium bis(trifluoromethanesulfonyl)imide(LiTFSI) solution was added, then 60 μL of the HTL precursor solution was added to the glass substrate.
3.The substrate was firstly spun at 1000 rpm for 2 sec, then accelerated to5000 rpm in 4 sec, and further spun another 34 sec.

2.5. Evaporated metal electrode

1.Vapor deposition box was vacuumed until the vacuum level reaches 10−5 bar.
2.Metal electrode was evaporated to 60 nm at a rate of 10 Å per minute.

3. Results and discussion

3.1. Ultraviolet–visible spectroscopy (UV-vis) measurement

Ultraviolet-visible (UV-vis) spectra of materials were collected on a CARY-3600 UV-Vis spectrophotometer with a range of 400-800 nm, a step size of 1 nm and a resolution of ≤ 1 nm.

DOI: 10.54254/2755-2721/2026.MH30175

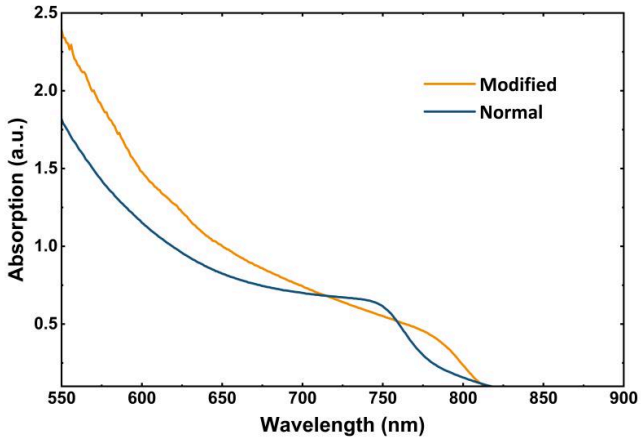


Figure 4. UV-Vis spectra of the normal (dark blue) and modified (orange) perovskite cells

The UV-Vis absorption spectra (Figure 4) shows that the modified perovskite cells exhibit in general higher absorption value compared to normal perovskite cells. This spectrum clearly shows that the incorporation of FA into the perovskite lattice effectively led to a red shift in their absorption edge, and an overall increase of light absorption efficiency exceeding 800 nm.

3.2. Photoluminescence (PL) characterization

The FLS-980 fluorescence spectrometer, equipped with a Xenon lamp as an excitation source, is used to measure PL. The excitation wavelength is selected in the strong absorption region of the perovskite at 530 nm, and the emission scanning range covers the band-edge emission (e.g., 650 - 900 nm). The PL peak energy of direct bandgap perovskites is approximately equal to the bandgap, the PL peak of modified and normal perovskites are at 805 nm and 767 nm correspondingly, exhibiting a red shift, which is in accordance with the properties reflected by the UV-vis absorption spectrum.

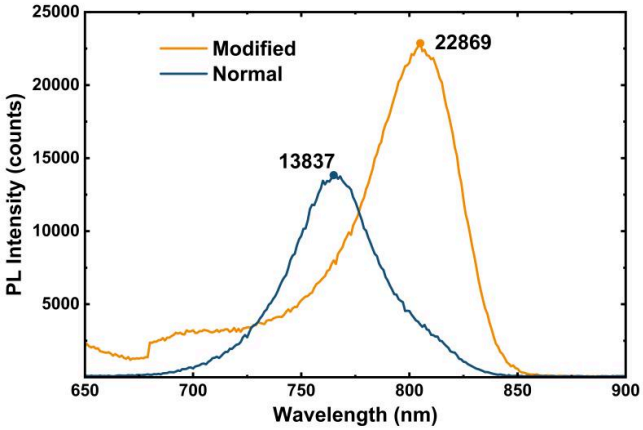


Figure 5. PL Graph of the normal (dark blue) and modified (orange) perovskite

Cells.As shown in Figure 5, for the Modified sample, within the range of 650 900 nm, the PL intensity is significantly higher than that of the Normal Sample (up to 2.2 × 104 Counts), indicating a higher carrier radiative recombination efficiency, which indicates for better energy converting

DOI: 10.54254/2755-2721/2026.MH30175

ability of the Modified sample. The peak occurs around 780 - 800 nm, and the intensity gradually decreases after >800 nm. The photoluminescence spectrum of the Modified cells shows a left skewed pattern, which indicates that the modified cells play an inhibitory role in the left tail.

3.3. Scanning electron microscope surface morphology characterization

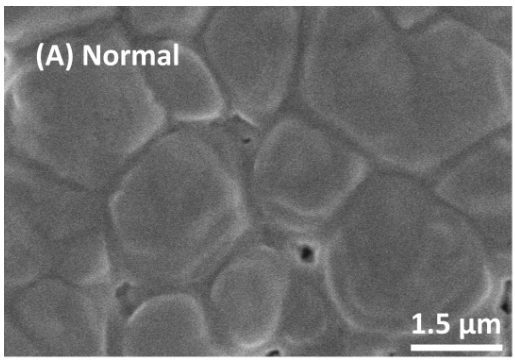


Figure 6. SEM images of perovskite films

The SEM images (Figure 6) of the two different samples show notable differences. The Normal film displays smaller grains, whereas the Modified film exhibits larger, more compact grains with much fewer pinholes. This grain enlargement enhances carrier transport pathways and reduces recombination at grain boundaries. More importantly, the reduced defect density in the Modified film corresponds to a stronger resistance against ion migration, as grain boundaries are typical channels for ion movement in perovskite lattices.

3.4. X-Ray Diffraction (XRD) measurement

Both sets of data from the modified and the normal cells were collected using a Cu target (λ = 1.5406Å), with an applied voltage of 40kV and a current of 30mA. The scanning range was 2θ = 10° to 50°, with a step size of 0.02°. The location of the peaks in the XRD graph wasn't showing an obvious move from the normal cells to the modified cells (Figure 7). The most prominent diffraction peaks appear at 2θ = 18.76° and 21.88°. The modified cells, compared to the normal ones, exhibit decreased full width at half maximum (FWHM), reflecting an increment in crystallinity and grain size, which correlates well with the SEM results.

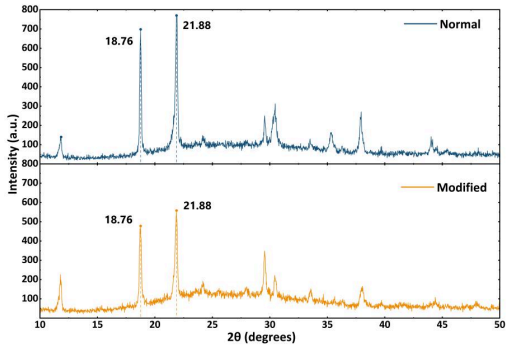


Figure 7. XRD graph of the normal (dark blue) and modified (orange) perovskite cells

DOI: 10.54254/2755-2721/2026.MH30175

3.5. Current density and voltage measurement

Using the AM 1.5G solar simulator, calibrate the light intensity to 100 mW/cm^2 (corresponding to standard one sun illumination), with a uniformity error of less than 2%. Control the temperature of the test environment temperature at 25±1 ℃ to avoid the influence of thermal effects on device performance. Source meter with a scanning rate typically in the range of 0.1 V/s. Conduct forward ($0 \rightarrow V_{oc}$) and reverse ($V_{oc} \rightarrow 0$) scans from -0.3 V to 1.2 V, 10 mV/step, separately to evaluate the lag effect.

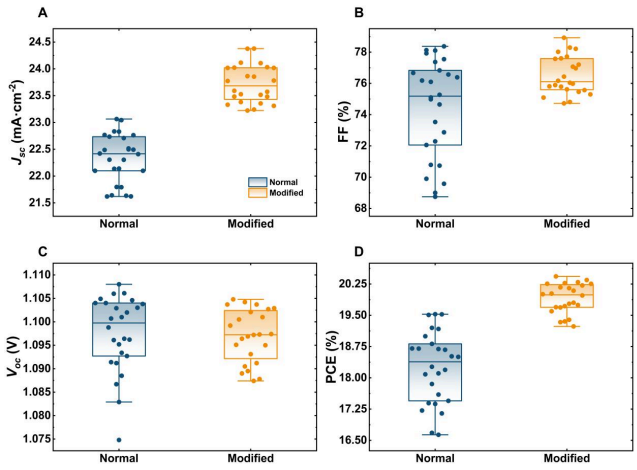


Figure 8. Photovoltaic analysis of normal (dark blue) and modified (orange) perovskites. (A) short-circuit current intensity, (B) fill factor, (C) open circuit voltage, and (D) power conversion efficiency

According to statistical analysis and as shown in Figure 8, the performance of the modified cells is significantly better than that of the normal cells, with a higher mean power conversion efficiency (19.91 ± 0.36 for the modified cells versus 18.25 ± 0.86 for the normal cells) and also a higher median power conversion efficiency (19.99 for the modified cells versus 18.38 for the normal cells). Modified devices also show a higher J_{sc} (~ 23.5−24.3 mA·cm−2) compared to Normal devices (~ 22.0−22.8 mA·cm^{-2}). This indicates that the modified devices are converting more photons into charge carriers and transporting them to the electrodes efficiently. In other words, the modified devices are harvesting more solar energy per unit area, in agreement with what the uv-vis absorption spectrum has shown. In addition, modified devices have a tighter distribution (IQR = 1.99 for modified perovskites compared to IQR = 4.77 for the normal perovskites) and slightly higher median fill factor (76.11%) compared to Normal (75.19%), meaning that the cell is operating closer to its ideal diode behavior, generating more carriers and also using them more efficiently. The V_{oc} of the modified perovskites (~ 1.092−1.105), however, are slightly lower than the normal perovskites (~ 1.092−1.108). In short, the modified cells demonstrate improved shot-circuit current density (~ 5.7% increment of median), fill factor (~ 1.2% increment of median) and power conversion efficiency (~ 8.8% increment of median) while maintaining comparable open-circuit voltage compared to normal samples.

3.6. Open Circuit Voltage Decay (OCVD)

The Open Circuit Voltage Decay (OCVD) graph (Figure 9) has compared the carrier recombination dynamics of the MA (normal) and $MA_{0.15}FA_{0.85}$ (modified) perovskite devices. In both tests, initial

DOI: 10.54254/2755-2721/2026.MH30175

voltage corresponding to the steady-state photovoltage under illumination was maintained prior to the removal of light, and the subsequent decay which reflects how quickly photogenerated carriers recombine after the light is switched off.

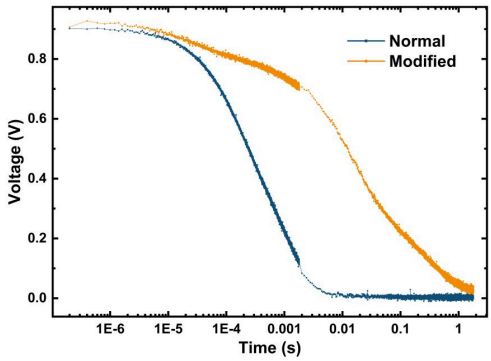


Figure 9. Open Circuit Voltage Decay graph of the normal (dark blue) and modified (orange) perovskite cells

The normal device (dark blue curve) shows a rapid voltage drop within approximately 0.1 ms - 10 ms, which indicates a high recombination rate and short carrier lifetime. In contrast, the modified device (orange curve) exhibits a substantially slower decay over the same time range. This signifies reduced recombination losses and prolonged carrier lifetimes. Notably, the modified perovskites also show an abnormally slow decay process after approximately 10 ms, which can be attributed to the delayed response of residual ion migration within the perovskite lattice. Both the improvement can be attributed to the incorporation of the larger FA cation, which introduces a steric effect within the perovskite lattice. This steric effect stabilizes the crystal structure, reduces defect density, and suppresses recombination pathways. The bulkier FA ions hinder ion migration by creating higher energy barriers for mobile species, further prolonging charge carrier lifetimes, enhancing both the efficiency and long-term stability of the devices. Hence, the OCVD results clearly demonstrate that FA-rich composition both substantially suppresses recombination compared to pure MA and hinders the ion migration process.

4. Conclusion

Ion migration remains a critical challenge in perovskite photovoltaic (PVK) devices. It is essential to understand the underlying mechanism of ion migration, which allows strategies to be developed in order to mitigate the adverse effects generated by the migration. In this study, we explored the impact of incorporating large cations, specifically the partial substitution of MA^+ with FA^+, on perovskite films. The modified perovskites exhibited enhanced PCE. Characterization through PL and OCVD demonstrated that the steric effect introduced by the larger FA cations effectively reduces defect density and slows carrier recombination. Also, the modification alters crystal growth and grain morphology, creating more compact grains that hinder ion migration. These results confirm that the spatial steric effect from larger cations is a practical means to suppress ion migration and enhance device performance.

Overall, this study highlights that precise compositional engineering can regulate ion migration in perovskites, offering a pathway to more stable and efficient devices. Future research can focus on the systematic exploration of other large organic cations, the development of hybrid structures, and advanced in situ characterization to further elucidate ion migration pathways, develop and enhance

DOI: 10.54254/2755-2721/2026.MH30175

the performance of perovskites, and ultimately bridge the gap between laboratory optimization of perovskites with vast commercial production.

References

[1] Akihiro Kojima et al. “Organometal halide perovskites as visible-light sensitizers for photovoltaic cells”. In: Journal of the American Chemical Society 131.17 (2009), pp. 6050–6051.
[2] Martin A. Green et al. “Solar Cell Efficiency Tables (version 66)”. In: Progress in Photovoltaics: Research and Applications 33.7 (May 2025), pp. 795–810.
[3] National Renewable Energy Laboratory. Best Research-Cell Efficiency Chart. July 2025.
[4] Feng Hao et al. “Anomalous band gap behavior in mixed Sn and Pb perovskites enables broadening of absorption spectrum in solar cells”. In: Journal of the American Chemical Society 136.22 (2014), pp. 8094–8099.
[5] Loredana Protesescu et al. “Nanocrystals of cesium lead halide perovskites (CsPbX3, X = Cl, Br, and I): novel optoelectronic materials showing bright emission with wide color gamut”. In: Nano letters 15.6 (2015), pp. 3692–3696.
[6] Rui Wang et al. “Opportunities and challenges of lead-free perovskite optoelectronic devices”. In: Trends in Chemistry 1.4 (2019), pp. 368–379.
[7] Ramesh Kumar, Monojit Bag, and Sagar M. Jain. “Dual-edged sword of ion migration in perovskite materials for simultaneous energy harvesting and storage application”. In: iScience 26.11 (2023), p. 108172. issn: 2589-0042.
[8] Xiaolei Li et al. “Organic–inorganic copper (II)-based material: A low-toxic, highly stable light absorber for photovoltaic application”. In: The Journal of Physical Chemistry Letters 8.8 (2017), pp. 1804–1809.
[9] Tanzi Ahmed Chowdhury et al. “Stability of perovskite solar cells: issues and prospects”. In: RSC Advances 13.3 (2023), pp. 1787–1810.
[10] Zhenghong Dai et al. “Interfacial toughening with self-assembled monolayers enhances perovskite solar cell reliability”. In: Science 372.6542 (2021), pp. 618– 622.
[11] Huanping Zhou et al. “Interface engineering of highly efficient perovskite solar cells”. In: Science 345.6196 (2014), pp. 542–546.
[12] Enbing Bi et al. “Mitigating ion migration in perovskite solar cells”. In: Trends in Chemistry 3.7 (2021), pp. 575–588.
[13] Keyu Wei et al. “Perovskite heteroepitaxy for high-efficiency and stable purered LEDs”. In: Nature (2025), pp. 1–8.
[14] Jing Liang et al. “Nanometer-Resolved Mapping of Organic Cation Migration Behavior in Methylammonium Lead Halide Perovskites”. In: Angewandte Chemie International Edition 63.40 (2024), e202410557.
[15] Taeyong Kim et al. “Mapping the pathways of photo-induced ion migration in organic-inorganic hybrid halide perovskites”. In: Nature Communications 14.1 (2023), p. 1846.
[16] Xiayan Wu et al. “In Situ Monitoring of Nanocrystal Formation and Ion Migration in Lead Halide Perovskite Metal–Organic Framework Composites”. In: Advanced Optical Materials 12.3 (2024), p. 2301479.
[17] Yu Zhang et al. “Improved fatigue behaviour of perovskite solar cells with an interfacial starch–polyiodide buffer layer”. In: Nature Photonics 17.12 (2023), pp. 1066–1073.
[18] Hsinhan Tsai et al. “High-efficiency two-dimensional Ruddlesden–Popper perovskite solar cells”. In: Nature 536.7616 (2016), pp. 312–316.
[19] Boyao Zhang et al. “Inhibiting Ion Migration and Stabilizing Crystal-Phase in Halide Perovskite via Directly Incorporated Fluoride Anion”. In: Angewandte Chemie International Edition 137.1 (2025), e202413550.
[20] Dongmei He et al. “Universal Ion Migration Suppression Strategy Based on Supramolecular Host–Guest Interaction for High-Performance Perovskite Solar Cells”. In: Advanced Materials (2025), p. 2505115.
[21] Huachao Zai et al. “Ion migration in halide perovskite solar cells: Mechanism, characterization, impact and suppression”. In: Journal of Energy Chemistry 63 (2021), pp. 528–549.